Brighten or Harm: Light Pollution Risk Assessment and Prevention

Han Li [1, *], Yuxin Tian [2], Yang Xing [2]

[1] Faculty of Science, Beijing University of Technology, Beijing, China, 100124

[2] Beijing Dublin International College, Beijing University of Technology, Beijing, China, 100124

* Corresponding author: alice.lihan@icloud.com

[#]These authors contributed equally.

Abstract. Light pollution harms health and the environment, but global assessments only measure light pollution levels, lacking a comprehensive evaluation of its risk. The evaluation model was developed to assess direct and indirect influences with 11 factors, ensuring mutual independence through the KMO test, assigning weights via the AHP model, and applying it to 49 cities globally based on varying urban levels. Using the TOPSIS model, we calculated comprehensive scores for each city and applied K-Means clustering to categorize scores into different levels. Four distinct sites were chosen to validate the model's reliability. By utilizing pertinent data for each indicator, the established model was employed to assess the light pollution risk levels at these locations. Subsequent to this investigation, three intervention strategies were formulated as potential measures to mitigate light pollution, accompanied by a comprehensive analysis of their possible impacts. Finally, 49 cities were classified into five light pollution levels, affirming the practicality of the model. The analysis led to the identification of three intervention strategies: "Material Optimization," "Enhanced Artificial Application," and "Public Education and Awareness."

Keywords: Light Pollution, TOPSIS Model, AHP Model, Intervention Strategies.

1. Introduction

Light pollution, arising from the indiscriminate use of artificial light, has emerged as a contemporary environmental challenge, posing threats to human health, safety, and ecological balance [1]. Recognizing the need for a comprehensive approach to evaluate and address the multifaceted impacts of light pollution, this study aims to establish a criterion considering various factors and develop models for assessing the risk level of light pollution in specific regions. The dynamic nature of light pollution, influenced by diverse territorial features, requires a tailored assessment model to account for its varying impacts. Moreover, the implementation of policies to curb light pollution may yield both positive and negative consequences, necessitating a nuanced intervention strategy. This article undertakes a series of tasks to contribute to the understanding and mitigation of light pollution.

The significance of this research is underscored by the growing body of literature emphasizing the detrimental effects of light pollution on both human and environmental well-being. Researchers have observed the disturbance of biological rhythms of flora and fauna [2]. As an emerging environmental concern, the need for an integrative assessment model and targeted intervention strategies is evident. The gaps in existing research underscore the importance of this study in providing a comprehensive framework for evaluating and mitigating light pollution.

One innovative aspect of this study involves the quantification of light pollution using LuoJia remote sensing satellite imagery. The adoption of a gridded approach allows for a systematic and detailed analysis, providing essential experimental data. By incorporating this unique dataset into the assessment model, the research aims to enhance the accuracy and applicability of the findings, contributing to the broader understanding of light pollution dynamics.

To address the multifaceted challenges outlined above, this article outlines a structured approach. Firstly, a model reflecting the risk level of light pollution will be developed based on relevant literature, rational indicators, and collected data. Subsequently, the model will be applied to diverse locations, integrating existing data to measure the light pollution risk level. Building upon these assessments, the study will propose intervention strategies tailored to each region, considering potential positive and negative impacts. The effectiveness of these strategies will be evaluated by comparing the light pollution risk levels before and after implementation.

2. Indicator Selection

2.1. Selection criteria

The factors that affect the risk level of light pollution in a region are diversified, which can be precisely divided into two main aspects: direct impact indicators and indirect impact indicators. McKinsey logic tree analysis is used to make a selection of necessary, proper, and accessible indicators of each aspect to estimate the light pollution risk level relatively accurate for the specific location. The data of selected indicators will be processed and presented as score levels. The selected indicators are shown in table 1 and table 2.

2.2. Direct Impact Indicator

Indicators that directly reflect the light pollution index are often derived from astronomical observations. However, more complex quantifiable data, such as the Sky Quality Meter (SQM), can be more effective, even though they may have some limitations[3]. The indicators in the following table1 can directly reflect the level of light pollution or directly affect the illumination of light. The data of some indicators are not presented in the form of scores. The scoring procedure of these indicators will be according to the structure and analysis of the data.

Table 1. Direct Impact Indicator Definition

Name	Full Name	Explanation
SIQD	Satellite Image Qualified Data	Luojia 1-01 satellite's high-res night illumination images offer direct, de- tailed insights into light pollution levels for accurate assessment.
BS	Bortle Scale	Astronomical night sky brightness scale, crucial for assessing light pollution impact on celestial visibility.
APM	Atmospheric Particulate Matters	Categorizing pm2.5 and pm10 based on Air Quality Index informs on aerosol content, contributing to visible light scattering and light pollution.
O3	Ozone Content	Atmospheric ozone levels correlate with light pollution, reflecting inhibitory effects from artificial light sources.
RALS	Ratio of artificial light bright- ness to sky brightness [4]	Artificial light pollution contributes to the overall background against which astronomical objects are observed [5]. Globally consulted indicator gauges light pollution by comparing artificial and natural sky brightness ratios.
SQM	Sky Quality Meter	A precise instrument measuring sky brightness, SQM quantifies the quality of the night sky. Essential for evaluating light pollution impact on astronomical observation.

2.3. Indirect Impact Indicators

In order to effectively assess the risk level of light pollution, considering the indicators that indirectly conduct impact light pollution and the factors that may be potentially affected by light pollution is necessary. For instance, the use of artificial lighting has the potential leading to significant and possibly adverse impacts on biological rhythms [6]. The following table2 the indirect factors that we feel need to be considered and their definitions.

Table 2. Indirect Impact Indicators Definition

Name	Full Name	Explanation
GDP	Gross Domestic Product	Key economic indicator reflecting a region's development, indirectly influencing light pollution through artificial light use.
Population & Urbanization	Population & Urbanization	Population size and urbanization impact artificial light usage, affecting the scope and severity of light pollution, with urbanization amplifying light reflection.
WAS	Whether adjacent to the sea	Coastal cities score higher due to in-creased lighting demands from ship activities, humid climate, and water mist content.
LS	Living Species [7]	Light pollution threatens human health and wildlife, impacting biodiversity. Biological rhythms of some bird species are affected by light pollution as well. [8]

2.4. Innovation in Methodology

Satellite Image Qualified Data (SIQD): Quantifying light pollution faces challenges due to limited direct data. Despite efforts to gather relevant atmospheric information, there remains a data gap. Since 1970, the assessment of the light pollution index through satellite imagery has become increasingly applicable. However, commonly used satellites such as meteorological satellites produce images with limited clarity. The Luojia 1-01 satellite offers a solution, providing high-resolution night illumination images.

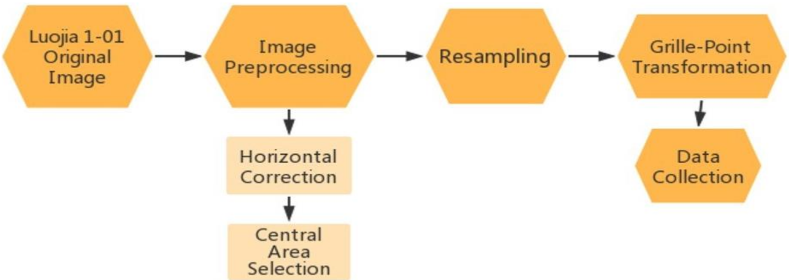

Figure 1. Flow chart of data processing

Through preprocessing, resampling, and Grille-Point transformation using ArcGIS, we extract and score data above brightness thresholds, completing the quantization of remote sensing images. Refer to Fig1 for the detailed processing procedure and example and Fig2.

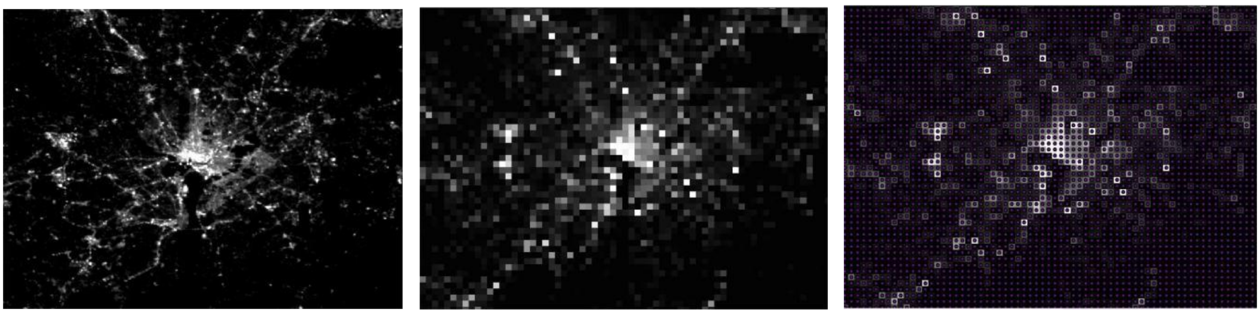

(a) Original Image (b) After Resampling (c) After Grille-Point Transformation

Figure 2. Processing Procedure of Washington D.C.

3. Model Building

3.1. KMO Test

The Kaiser–Meyer–Olkin test (KMO) is a statistical measure. The test measures sampling adequacy for each variable in the model and the complete model. The KMO statistic is a measure of the proportion of variance among variables that might be common varian [9].T he smaller the value, the weaker the correlation between variables. We calculated KMO=0 through the formula of the 11 indicators selected. These 11 indicators are highly independent.

$$KMO = \frac{\sum\sum_{i\neq j} r_{ij}^2}{\sum\sum_{i\neq j} r_{ij}^2 + \sum\sum_{i\neq j} \alpha_{ij}^2} (i, j = 1,2 \cdots k) \tag{1}$$

3.2. Determine the Weight of Indicators

The primary method employed to ascertain weights is the Analytic Hierarchy Process (AHP), recognized for its precision in quantifying decision criteria weights and widely applied in various decision scenarios. AHP is an accurate approach for quantifying the weights of decision criteria, widely used in many decision situations [10]. In this analysis, the AHP method is utilized to determine the weights of different indicators. Two rounds of AHP were conducted to establish the weights for the two aspects of indicators, followed by determining the weights between these two aspects. Each AHP round underwent a consistency test, and the final weights were derived accordingly. The analytical steps are illustrated in Fig. 3.

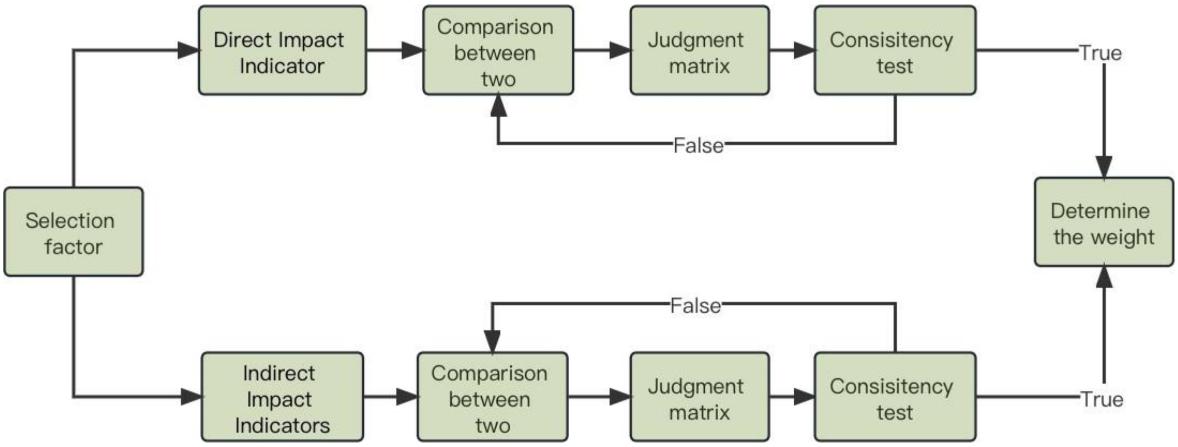

Figure 3. Process of AHP

3.2.1. Comparing Priorities between the Different Factors

After the AHP process, we considered the importance of the direct and indirect indicators to satisfy the following relationship:

Direct Impact Indicator: RAS ≈ SIQD > BS ≈ SQM > O_3 ≈ APM

Indirect Impact Indicator: GDP > Population ≈ Urbanization > LS > WAS

3.2.2. Computational Judgment Matrix

With the relationship discussed before, we get our judgment matrix like table 3 and table 4:

Table 3. Judgment matrix of direct factors

	BS	SQM	O_3	APM	RAS	SIQD
BS	1	1	5	4	1	$\frac{1}{2}$
SQM	1	1	4	3	$\frac{1}{2}$	$\frac{1}{2}$
O_3	$\frac{1}{5}$	$\frac{1}{4}$	1	1	$\frac{1}{7}$	$\frac{1}{7}$
APM	$\frac{1}{4}$	$\frac{1}{3}$	1	1	$\frac{1}{6}$	$\frac{1}{6}$
RAS	1	2	7	6	1	1
SIQD	2	2	7	6	1	1

Table 4. Judgment matrix of indirect factors

	GDP	Population	Urbanization	LS	WAS
GDP	1	3	2	7	4
Population	$\frac{1}{3}$	1	$\frac{1}{2}$	6	4
Urbanization	$\frac{1}{2}$	2	1	7	4
LS	$\frac{1}{7}$	$\frac{1}{6}$	$\frac{1}{7}$	1	$\frac{1}{2}$
WAS	$\frac{1}{4}$	$\frac{1}{4}$	$\frac{1}{5}$	2	1

3.2.3. Consistency Test

We calculate the eigenvectors and the maximum eigenvalues λmax based on the above matrix. The next step is to calculate the value of CI according to λmax, and then calculate CR according to the ratio of CI and RI to complete the consistency test.

$$CI = \frac{\lambda_{max} - n}{n-1} \tag{2}$$

$$CR = \frac{CI}{RI} \tag{3}$$

Direct Impact Indicator: where RI = 1.25 when n = 6. For the above judgement matrix, we obtain. CR = 0.0022 < 0.1, thus the judgement matrix is acceptable.

Indirect Impact Indicator: where RI = 1.11 when n = 5. For the above judgement matrix, we obtain. CR = 0.039 < 0.1, thus the judgement matrix is acceptable.

3.2.4. Determine the Weight

Through consistency test, we gained the weight of the Direct Impact Indicator: RAS (30.148%), SIQD (26.589%), BS (18.839%), SQM (15.413%), APM (4.668%), O3 (4.072%) and the weight of the Indirect Impact Indicator: GDP (40.386%), Population (19.124%), Urbanization (29.511%), LS (6.93%), WAS (4.048%).

At the same time, we use the same method to determine the weight between two aspects of. indicators. The weight of Determine the weight is 60 percent, and the weight of Indirect Impact Indicator is 40 percent. Then multiply each index of the weight calculated above by the weight of their categories respectively to get the final weight, as shown in the table 5.

Table 5. Distribution of Factors Contributing to Light Pollution

Factor	Percentage
Bortle Scale	16.15%
Ozone Content	11.80%
Ratio of artificial light to sky brightness	16.15%
GDP	11.80%
Population	7.64%
Living Species	0.16%
SQM	18.09%
Atmospheric Particulate Matters	9.24%
Satellite Image Qualified Data	2.80%
Urbanization	2.77%
Whether adjacent to the sea	0.28%

3.3. Calculate the Score

In order to make our model possess expansive practicality, we selected 50 cities of different grades all over the world according to the ranking conducted by Globalization and World Cities (GaWC) [11]. With the collected data of each city in these 11 indicators, using TOPSIS model to calculate the comprehensive score of each city. Firstly, creating a matrix xnm which contain data for all indicators for 50 cities, with n representing the number of countries and m representing the number of indicators.

Most of the indicators we selected were the minimal indicator, which has the positive correlation with the mitigation of the light pollution risk level. Therefore, we get a new matrix ynm by converting the index to the maximum indicator size through the formula.

In order to eliminate the influence of different dimensions of indicators, we standardize the matrix and establish a standardized matrix znm. The standardized formula is as follows:

$$z_{ij} = \frac{x_{ij}}{\sqrt{\sum_{i=1}^{m} x_{ij}^2}} \tag{4}$$

First, the maximum and minimum values are defined according to the standardized matrix.

$$\begin{cases} Z^+ = (Z_1^+, Z_2^+, \cdots Z_m^+) = \\ (max\{z_{11}, z_{21}, \cdots z_{n1}\}, max\{z_{12}, z_{22}, \cdots z_{n2}\}, \cdots max\{z_{1m}, z_{2m}, \cdots z_{nm}\}) \\ Z^- = (Z_1^-, Z_2^-, \cdots Z_m^-) = \\ (min\{z_{11}, z_{21}, \cdots z_{n1}\}, min\{z_{12}, z_{22}, \cdots z_{n2}\}, \cdots min\{z_{1m}, z_{2m}, \cdots z_{nm}\}) \end{cases} \tag{5}$$

The next step is to define the distance between the i − th(i = 1,2,⋯ ,n) evaluation object and the maximum (minimum) value.

$$\begin{cases} D_i'^+ = \sqrt{\sum_{j=1}^{n} \left(Z_j^+ - z_{ij}\right)^2} \\ D_i'^- = \sqrt{\sum_{j=1}^{n} \left(Z_j^- - z_{ij}\right)^2} \end{cases} \tag{6}$$

Finally, the final composite score of each city can be calculated according to the formula.

$$S_i = \frac{D_i'^-}{D_i'^+ + D_i'^-} \tag{7}$$

Here are our results. Due to the large sample size, only the top 10 cities are shown in the table6 below.

Table 6. City ranking

City	Composite score index	Sort
Tokyo	0.79	1
Singapore	0.68	2
Seoul	0.63	3
Los Angeles	0.61	4
New York	0.60	5
Moscow	0.59	6
Houston	0.57	7
Wuhan	0.55	8
Hangzhou	0.55	9
Sydney	0.54	10

3.4. Rank Determination

According to the overall score of each city, we use K-mean Cluster Method to classify cities into five levels from light to heavy. Depending on the generated level, evaluation of the light pollution risk level of specific location is able to obtained.

Firstly, Euclidean distance formula is used to calculate the distance between two sample points.fiα, fjα are comprehensive evaluation indexes based on TOPSIS.

$$d_{ij} = \sqrt{\sum_{\alpha=1}^{p} \left(f_{i\alpha} - f_{j\alpha}\right)^2} \qquad (p = 1,2,\cdots,49) \tag{8}$$

Based on the comparison of the clustering trees, which is shown in Fig4. It is easy to tell by the degree of" flattening of the slope" that five groups of classes are the best number of clusters.

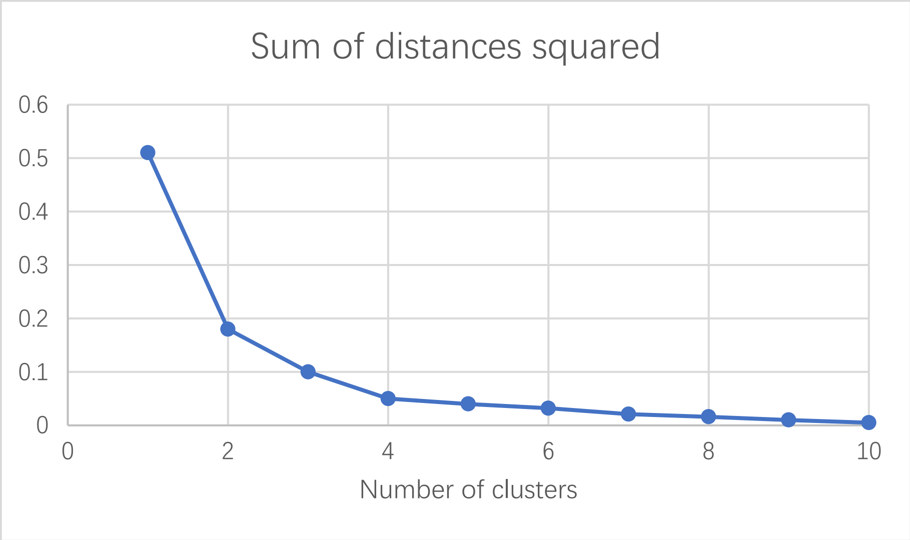

Figure 4. Cluster tree comparison graph

According to the data, the following table 7 is obtained by analyzing the difference of clustering categories.

Table 7. Analyzing the Difference of Clustering Categories

	Category 4 (n=18)	Category 2 (n=15)	Category 1 (n=10)	Category 5 (n=5)	Category 3 (n=1)	P
Composite score index	0.45 ±0.02	0.35 ±0.03	0.54 ±0.02	0.62 ±0.04	0.79 ±nan	0.000**

According to the results of the analysis of variance, for the comprehensive score index of the variable, the significance P value is 0.000, showing significance at the level. The null hypothesis is rejected, indicating that the comprehensive score index of the variable has a significant difference between the categories divided by the cluster analysis.

The frequency of each cluster category was analyzed according to clustering summary. According to the data clustering category annotation, each sample data can be classified into which category.

Table 8. Caption for the table

Clustering category	Frequency	Percentage
Clustering category—1	10	20.41%
Clustering category—2	15	30.61%
Clustering category—3	1	2.04%
Clustering category—4	18	36.74%
Clustering category—5	5	10.20%
Sum	49	100.0

Finally, light pollution risk levels are divided into 5 categories according to the proportions shown in the table8. At the same time, we also rated 49 sample cities, as shown in the figu9 below.

Table 9. City Light Pollution Level

City	Level	City	Level	City	Level	City	Level
Tokyo	5	Orlando	3	Berlin	2	Denver	2
Singapore	4	Washington	3	Fuzhou	2	Kobe	1
Seoul	4	Ho Chi Minh	3	Wuxi	2	Borussia Dortmund	1
Los Angeles	4	Ottawa	3	Macau	2	Sheffield	1
New York	4	Felix	2	Lyon	2	Omaha	1
Moscow	4	Qingdao	2	Zhuhai	2	Cleveland	1
Houston	3	Ningbo	2	Santiago	2	Quebec	1
Wuhan	3	Kyoto	2	Seattle	2	Nice	1
Hangzhou	3	Salt Lake City	2	Munich	2	Haikou	1
Sydney	3	Taiyuan	2	Wellington	2	Baltimore	1
Boston	3	Dublin	2	Cairo	2	Lille	1
Doha	3	Minsk	2	Atlanta	2	Kansas	1

4. Application of Light Pollution Risk Level Assessment Model

4.1. Location Selection

In the selection of the four locations, we possessed multiple of principles, which including but not limited to: The typicality of the location, the selected region should not have the characteristics that do not belong to the region. Comprehensiveness of data. For example, Yellowstone's geological history creates diverse habitats for birds [12]. It is desirable that the selected sites provide comprehensive data to ensure accurate assessment.

Based on specific criteria, we selected these locations based on specific criteria: Yellowstone National Park of United States for protected land, Sweet Lips town of United States for rural community, Changzhi section of China for suburban community, and Beijing of China for urban community.

4.2. Data Processing

We assigned the selected urban community, suburban community, rural community, and protected land as B1, B2, B3, and B4 respectively.11 indicators of each location were collected separately and following matrix $(b_{ij})4\times11$ was generated.

Based on the existing normalized data in task 1, conducting normalization of the indicator matrix of B1–B4 then the matrix c_{ij} is obtained in following.

$$c_{ij} = \frac{b_{ij}}{\sqrt{\sum_{i=1}^{m} a_{ij}{}^2}} \tag{9}$$

The weight $w = (w_1, w_2 \cdots w_n)$ of indicators acquired by the model is used to calculate the comprehensive indicator index y_{ij}.

$$y_{ij} = w_{ij} \times c_{ij} \tag{10}$$

Then the positive and negative ideal distance of the i-th location is able to carried out.

$$\begin{cases} D_i'^{+} = \sqrt{\sum_{j=1}^{n}\left(x_j^{+} - y_{ij}\right)^2} \\ D_i'^{-} = \sqrt{\sum_{j=1}^{n}\left(x_j^{-} - y_{ij}\right)^2} \end{cases} \tag{11}$$

Calculate the comprehensive evaluation index:

$$f_i'^{*} = \frac{D_i'^{-}}{D_i'^{-} + D_i'^{+}} \tag{12}$$

At last, based on the classified central value of the sample data at each level determined in Task 1, the distance between the new data $f_i'^{*}$ and each data in the original sample dataset is calculated by using the KNN approach.

$$d_{ij} = \sqrt{\sum_{\alpha=1}^{p}\left(f_{i\alpha} - f_{j\alpha}\right)^2} \qquad (p = 1,2,\cdots,49) \tag{13}$$

Sort the obtained distance d_{ij} (ascending order) which represents the distance to the central point of each risk level, then finally determine the light pollution risk level of the location.

4.3. Result

Based on the above calculation process, we obtained the light pollution risk level of four locations. They are respectively Yellowstone National Park−Level 1, Sweet Lips Town−Level 1, changzhi section−Level 3, and Beijing−Level 5, which is in line with our expectations.

5. Intervention Strategies

The mitigation of artificial light reflection in urban architecture, particularly polarized light pollution (PLP), requires strategic policies focusing on building materials optimization [13]. In high-traffic urban areas, careful selection of non-reflective materials is crucial to reduce the risk of traffic accidents caused by light pollution. When utilizing glass curtain walls, a comprehensive analysis considering environmental factors, climate, functionality, and planning requirements is essential, with rigorous certification processes ensuring suitability. To enhance the effectiveness of glass and reflective materials, a preference for rough surfaces or light-absorbing materials is advised, coupled with research for innovative glass materials. Addressing excessive artificial light use involves refining irradiated fixed light sources, reducing reflections, and limiting propagation distance, particularly in large facilities. Additionally, a reduction in LED lights and white light source, strategically lowering their duration and frequency on high-rise structures, and selectively deactivating light strips on buildings can effectively mitigate light pollution [14]. The broad scope of the light pollution issue necessitates raising awareness among the public through tailored education and outreach initiatives, disseminating information through various channels. This collective approach aims to foster a more judicious use of artificial lighting, mitigating public exposure to light pollution and its associated harms.

6. Conclusion

In the course of this study, 49 cities were categorized into five groups according to differing degrees of light pollution. The effectiveness of the proposed model was then evaluated through an analysis of light pollution risk levels in four distinct locations characterized by unique attributes: Yellowstone National Park (Level 1), Sweet Lips Township (Level 1), the Changzhi section (Level 3), and Beijing (Level 5). This analytical approach has contributed to an enriched comprehension of light pollution dynamics, leading to the formulation of three specific intervention strategies tailored to address identified concerns.

The model presented herein is versatile and capable of addressing an array of risk grading challenges beyond light pollution, including water, air, and noise pollution—all of which are broadly applicable to grading issues. Moreover, we have proposed three intervention policies for light pollution. These policies are designed to be practical and effective for both urban and rural contexts, with marked differences, providing sound and actionable plans to mitigate real-world light pollution.

Nevertheless, the current model has certain limitations. It requires the input of 11 index values for grade calculation, necessitating a substantial amount of data, which complicates the search process. Moreover, with current technologies, measuring the color temperature difference across different regions poses challenges, which may affect the accuracy of the grading outcomes.

Future technological advancements are anticipated to refine the model. By increasing the number of light pollution-related indicators and employing techniques such as factor analysis or principal component analysis, we could streamline data requirements, thereby simplifying the application of the model and enhancing its practical utility.

References

[1] Falchi, F., Bará, S., 2023. Light pollution is skyrocketing. Science, 379, pp. 234 - 235.

[2] Pérez Vega, C., Zielinska-Dabkowska, K. M., Schroer, S., Jechow, A. & Hölker, F. (2022) 'A systematic review for establishing relevant environmental parameters for urban lighting: Translating research into practice', Sustainability, 14 (3), 1107.

[3] Deverchère, P. et al., 2022. Towards an absolute light pollution indicator.

[4] Falchi, F. et al., 2016. The new world atlas of artificial night sky brightness. Science Advances, 2 (6), e1600377.

[5] Barentine, J. C. (2022) 'Night sky brightness measurement, quality assessment and monitoring', Nature Astronomy, 6 (10), pp. 1120 - 1132.

[6] Raap, T., Pinxten, R., Eens, M., 2015. Light pollution disrupts sleep in free-living animals. Scientific Reports, 5, 13557.

[7] Biological species. Available at: https://www.gbif.org/occurrence/search [Access date: 2023/2/16].

[8] Massetti, L., 2020. Drivers of artificial light at night variability in urban, rural and remote areas. Journal of Quantitative Spectroscopy and Radiative Transfer, 255, 107250.

[9] Wikipedia. Kaiser–Meyer–Olkin test. Available at: https://en.wikipedia.org/wiki/Kaiser [Access date: 2023/2/16].

[10] Wikipedia. Analytic hierarchy process. Available at: https://en.wikipedia.org/wiki/Analytic_hierarchy_process [Access date: 2023/2/16].

[11] City classification. Available at: https://www.10guoying.com/ [Access date: 2023/2/16].

[12] Landis, R. K. (2023). "Yellowstone's Birds: Diversity and Abundance in the World's First National Park." Princeton University Press.

[13] Lao, S. et al., 2020. The influence of artificial light at night and polarized light on bird-building collisions. Biological Conservation, 241, 108358.

[14] Esposito, T., Radetsky, L.C., 2023. Specifying Non-White Light Sources in Outdoor Applications to Reduce Light Pollution. LEUKOS, 19 (3), pp. 269 - 293.